

OPTICAL BUFFERING IN A BOTTLE MICRORESONATOR ON AN OPTICAL FIBER

Kalista Schauer^{a)} and Michael Pfenning^{b)}

¹United States Military Academy at West Point, West Point, New York 10996, USA

Corresponding author: ^{a)}*kalista.schauer@westpoint.edu*

^{b)}*michael.pfenning@westpoint.edu*

Abstract. Manufacturing highly efficient optical communications and computing devices requires designing dense integrated photonic circuits. Unfortunately, surface roughness of microscopic optical signaling devices results in light attenuation, decreasing the efficiency of the optical devices. A microscopic optical buffer would alleviate these issues; a potential solution is the Surface Nanoscale Axial Photonics (SNAP) platform. The SNAP platform operates because of the propagation of whispering gallery modes (WGMs) around the surface of an optical fiber. Because WGMs undergo slow axial propagation, they can be mathematically described by the one-dimensional Schrödinger equation. In this project, we calculate solutions to the effective wave equation to model the circulation of whispering gallery modes. We study the evolution of Gaussian-shaped wave pulses in a bottle microresonator on an optical fiber. By analyzing the propagation of WGMs within the bottle microresonator, we can examine the feasibility of creating a microscopic optical buffer for use in optical signal processing. In this project, we find analytical and numerical solutions to the effective wave equation, which is strikingly similar to the Schrödinger equation. We then use the numerical solutions to the effective wave equation to develop a model of the system in Mathematica.

INTRODUCTION

In 1935, Erwin Schrödinger introduced a thought experiment that applied quantum mechanics to a macroscopic system. In this gedanken, a cat is inside of a box that contains a radioactive particle and a vial of poison. If the particle decays, the poison is released and the cat dies. In quantum mechanics, the radioactive particle has two quantum states: decayed = $|\downarrow\rangle$ and undecayed = $|\uparrow\rangle$. Meanwhile, the cat also has two states: live = $|LL\rangle$ and dead = $|DD\rangle$. According to quantum mechanics, the system exists in a state of superposition where the cat is simultaneously alive and dead. This system is represented by the superposition wavefunction

$$\psi = \frac{1}{\sqrt{2}} [|\uparrow\rangle|LL\rangle + |\downarrow\rangle|DD\rangle] \quad (1)$$

Upon measurement of the system, if the particle is undecayed, then the cat will still be alive. However, if the particle has decayed, then the cat will certainly be dead.

Heisenberg's uncertainty principle states that one cannot precisely measure position and momentum simultaneously, with σ being the standard deviation for position and momentum, and is represented mathematically as

$$\sigma_x \sigma_p \geq \frac{\hbar}{2} \quad (2)$$

The time-dependent Schrödinger equation, written below, can be solved in order to find a particle's wavefunction:

$$i\hbar \frac{\partial \psi}{\partial t} = \frac{\hbar^2}{2m} \frac{\partial^2 \psi}{\partial x^2} + V\psi \quad (3)$$

Any observable within a given system can be described in terms of the wavefunction. Wavefunctions are given as a superposition of sinusoidal (pure time harmonic) vibrations. A group of vibrations with high quantum number m and

small quantum number differences can be used to represent a particle. The wave group, or density of a particle, described in quantum mechanics is always compact, whereas in classical optics, wave groups spread out into large regions over time. This characteristic applies to multidimensional oscillators as well. This is because wave packets under classical optics are described as a continuum, whereas under quantum mechanics, they are represented as discrete harmonic components.¹

An oft-studied problem in quantum physics is the infinite square well potential (Fig. 1). A particle in this potential is free, except at the boundaries of the square well. The boundaries of the potential constrain the particle and force it to oscillate. The potential is defined as

$$V(x) = \begin{cases} 0, & \text{if } 0 \leq x \leq a \\ \infty, & \text{otherwise} \end{cases} \quad (4)$$

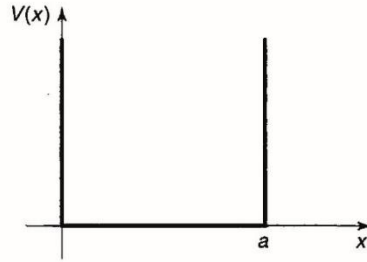


FIGURE 1. Infinite square well potential, Eq. (4).

A less idealized version of the infinite square well problem is that of the finite square well. In this problem, the potential is given by

$$V(x) = \begin{cases} -V_0 & |x| < 1 \\ 0 & |x| \geq 1 \end{cases} \quad (5)$$

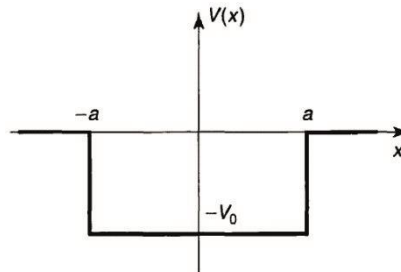


FIGURE 2. Finite square well potential.

Figure 2 is a depiction of Eq. (5).²

HARMONIC OSCILLATOR

In classical mechanics, a harmonic oscillator is often described as a system containing a mass m attached to a spring with force constant k . The motion of the spring-mass system is described by Hooke's law:³

$$-kx = m \frac{d^2x}{dt^2} \quad (6)$$

with the solution

$$x(t) = A \sin(\omega t) + B \cos(\omega t) \quad (7)$$

and potential energy

$$V(x) = \frac{1}{2} kx^2 \quad (8)$$

In quantum mechanics, the potential is written as

$$V(x) = \frac{1}{2} m\omega^2 x^2 \quad (9)$$

A quantum harmonic oscillator problem is solved by solving the Schrödinger equation for the above potential. The time-independent Schrödinger equation,³

$$\frac{d^2\psi}{dt^2} = -k^2\psi \tag{10}$$

describes the particle within the simple harmonic oscillator, with the general solution being

$$\psi(x) = A \sin(kx) + B \cos(kx) \tag{11}$$

and the possible energy values of the particle are quantized and given by²

$$E_n = \frac{n^2\pi^2\hbar^2}{2ma^2} \tag{12}$$

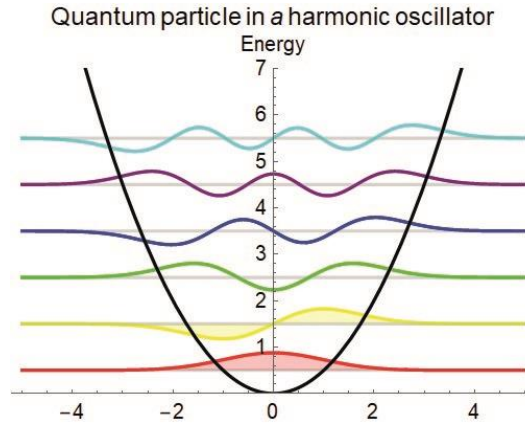


FIGURE 3. Mathematical model of a quantum particle in a harmonic oscillator.

The general solutions to the time-independent Schrödinger equation are visually similar to standing waves formed on a string with length a ; the potential well solutions have a ground state corresponding to the lowest energy and excited states corresponding to higher energies. Figure 3 shows the quantized energy states of a quantum particle within a harmonic oscillator. I generated this plot using Mathematica software.

Within a one-dimensional harmonic potential, a wave packet oscillates periodically. These oscillations are not distorted over time, a property that is desired when creating many applications. While creating a one-dimensional harmonic resonator is not viable, it is possible to mimic a quantum wave packet within a harmonic potential by examining optical pulses within bottle microresonators. A Surface Nanoscale Axial Photonics (SNAP) bottle microresonator is defined as a dielectric cylinder that has a nanoscale deformation.⁴ This fact is fundamental to this project.

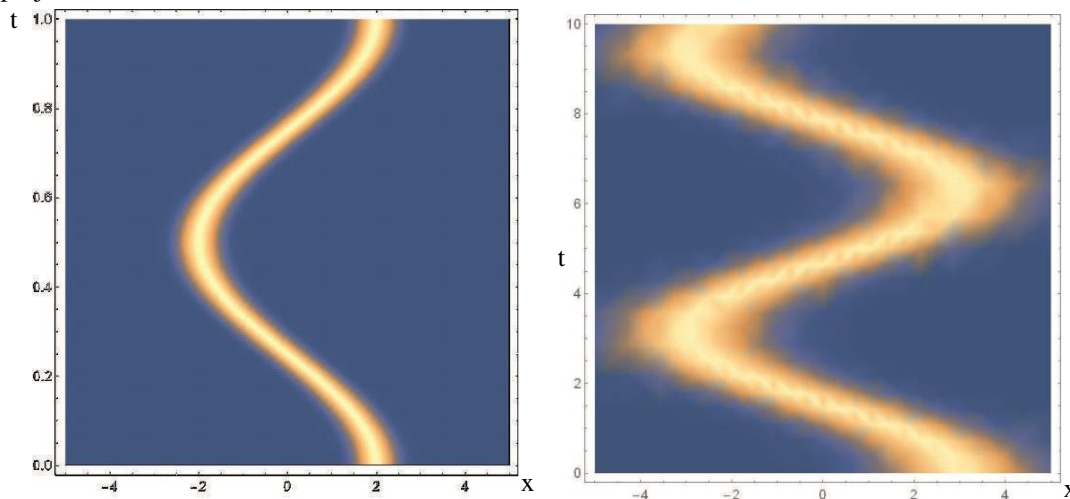


FIGURE 4. Left: A density plot of a stationary state of a wavefunction given in Schrödinger’s paper. Right: Mathematica density plot of a Gaussian wave in a harmonic oscillator.

WHISPERING GALLERY MODES

In open dielectric resonators, total internal reflection allows for closed trajectories of light. Within these resonators are circular optical modes known as whispering gallery modes (WGMs). WGMs are closed circular beams that occur because of total internal reflection. WGMs with low volume can achieve a high Q-factor, which is a dimensionless parameter that describes the level of damping of a resonator or oscillator. Simple geometries for open dielectric resonators include spheres, rings, or cylinders. The radius of curvature of these shapes is greater than several wavelengths, and the reflecting boundaries have high-index contrasts. Because of this, the Q-factor is only affected by material scattering or attenuation, which is caused by geometric imperfections such as surface roughness.⁵

Optical dielectric resonators with WGMs are a class of cavity devices that have useful properties, such as extremely high-power density, narrow spectral linewidth, and small mode volume. WGM resonators can be used to study quantum electrodynamics or nonlinear optical phenomena. In modern optics, optical resonators are not only fundamental to laser devices, but are also tools for optical filtering and attaining accurate measurements. However, bulk optical resonators have disadvantages concerning size, alignment, stability, and weight. Thus, research began in miniaturized optical resonators that contain dielectric structures with circular symmetry and support WGMs.⁶

SURFACE NANOSCALE AXIAL PHOTONICS (SNAP)

Current efforts to create highly efficient optical communications and computing devices require some form of dense photonic integration. However, microscopic devices contain surface roughness that leads to undesirable attenuation of light. A possible solution is the SNAP platform. The SNAP platform relies on the circulation of whispering gallery modes around the surface of an optical fiber. WGMs undergo slow axial propagation, which can be mathematically described by the one-dimensional Schrödinger equation. Manipulating the fiber radius on the nanoscale level causes variance in the modes of the WGMs. SNAP devices are extremely low loss, as SNAP devices have fiber surfaces with low surface roughness.⁷ Nanoscale variations of the radius of optical fibers result in an altered transmission spectrum. The evanescent field distribution of thin microfibers is very sensitive to nanoscale variations of the fiber radius. Optical fibers with larger radii are also sensitive to nanoscale variations of the fiber radius, and this effect is described by the slow propagation of WGMs along the axis of the fiber. Light in traditional silica optical fibers propagates along the interior core of the fiber. However, WGMs circulate around the surface of the fiber. The main premise of the SNAP platform is to manipulate WGM behavior by varying the effective fiber radius on an extremely small scale. Typically, WGMs can be excited by the evanescent field of a transverse microfiber. The SNAP platform is comprised of low-loss photonic integrated circuits that have sub-angstrom precision. The propagation of WGMs can be described by the Schrödinger equation, with energy proportional to variation of the wavelength and the potential $V(z)$ proportional to the variation of the radius.⁸

A focused CO₂ laser beam can modify the effective radius of the optical fiber on a nanoscale level. In order to achieve a predetermined variation of the radius, the laser beam is translated along the fiber. This method results in fabricated devices with sub-angstrom precision. This level of precision is more advanced than previous photonics technologies by two orders of magnitude.⁸ To employ SNAP structures, we use a whispering-gallery-mode nanobump microresonator (NBMR). A NBMR is fabricated by creating a nanoscale-high asymmetric deformation on the surface of the optical fiber. This method is then used to fabricate the SNAP structures. NBMRs cause the localization of WGMs near a geodesic (a closed and stable ray) on the surface of the fiber. Fabricating an asymmetrical nanoscale bump on the surface of the fiber allows for the creation of a microresonator with a high Q-factor and the ability to confine WGMs. Provided that the bump's height is small, the path will be stable and the WGMs will be fully localized. High nanobumps can lead to unstable geodesics. The aforementioned CO₂ laser beam is used to create a nanoscale variation in the effective fiber radius. The laser heats only one side of the fiber radius, leading to the asymmetry of the nanobump. The characteristic axial width of the fundamental whispering gallery mode, when localized in close proximity to a stable geodesic, is given by

$$z_w = \left(\frac{\lambda}{2\pi n_r} \right)^{1/2} \frac{(ar_0)^{1/2}}{(\Delta r_0 b)^{1/4}} \quad (13)$$

with height Δr_0 and widths a, b .⁹

CALCULATIONS

In this section, we examine the effective wave equation and calculate analytical solutions. The effective wave equation is very similar to the Schrödinger wave equation and differs only in terms of the constants. Thus, we can solve the effective wave equation as we would solve the Schrödinger wave equation. The effective wave equation is

$$i\mu \frac{\partial \psi}{\partial t} = -\frac{\partial^2 \psi}{\partial z^2} + V(x, t)\psi \quad (14)$$

Given the above wave equation and the initial profile of the wave at time $t = 0$, we can solve for the solution for all times $t \geq 0$ by modeling and solving the well-posed Cauchy problem. A well-posed problem is one that satisfies the following conditions: (1) the problem has a solution, (2) the solution is unique within a specific class of functions, and (3) the solution is dependent upon parameters and data, so that small changes in the boundary or initial conditions results in small changes in the solution.

There are two important assumptions to note. First, we assume a static potential. Second, we assume that the potential is in the physical shape of either a cylinder, mathematically represented by a finite square well potential, or a parabolic-shaped bead, mathematically represented by a harmonic oscillator potential.

An important consequence of the first assumption is that the given modes, which are

$$\psi_k(z, t) = u_k(z)e^{i\omega_k t} \cdot a_k \quad (15)$$

where $e^{i\omega_k t}$ represents the harmonic time dependence, imply the generic solution of

$$\Psi_k(z, t) = \sum_{\text{all modes } k} \psi_k(z)e^{i\omega_k t} \cdot a_k \quad (16)$$

where a_k is a Fourier coefficient.

We use the initial condition of $\Psi(z, 0)$ to determine the solution, giving

$$\Psi_k(z, 0) = \sum_{\text{all modes } k} \psi_k(z) \cdot a_k \quad (17)$$

Solving the remainder of this problem requires using Fourier analysis. To do so, it is necessary to define the inner product as

$$\langle f(x), g(x) \rangle = \int_{\text{all space}} f(x)\overline{g(x)}dx \quad (18)$$

For this specific problem, the inner product can be written as

$$\langle \Psi(z, 0), \psi_j(k) \rangle = \sum_{\text{all modes}} \langle \psi_k, \psi_j \rangle a_k \quad (19)$$

where j, k are arbitrary parameters. The inner product can also be represented as

$$\langle \Psi(z, 0), \psi_j(k) \rangle = \sum_{\text{all modes}} \delta_{k,j} a_k \quad (20)$$

where $\delta_{k,j}$ is the Kronecker delta, defined as

$$\delta_{k,j} = \begin{cases} 0, & k \neq j \\ 1, & k = j \end{cases} \quad (21)$$

Because the Kronecker delta gives a nonzero result only when $k = j$, the only surviving term of the inner product is

$$\langle \Psi(z, 0), \psi_j(k) \rangle = a_j \quad (22)$$

Thus, the analytic solution to the well-posed Cauchy problem is

$$a_k = \langle \Psi(z, 0), \psi_j(k) \rangle \quad (23)$$

$$\Psi(z, t) = \sum_{\text{all modes}} a_k \psi_k(z)e^{i\omega t} \quad (24)$$

When the assumptions do not hold true, such as with beads of different shapes or time-changing potentials, it is necessary to abandon the analytic solution for a numerical simulation calculated on a computer.

RESULTS

Figure 6, middle, simulates a Gaussian pulse in an idealized infinite square well. This Mathematica-generated plot is two-dimensional and simulates the pulse as the light pulse propagates radially in the microresonator. This image shows that the Gaussian pulse reflects off the boundary of the microresonator and then interferes with itself, causing the interference patterns shown past $t = 0.2$. As the simulation uses an infinite square well, the only interference occurs from the pulse itself. The pulse only reflects off the boundary of the microresonator, and no part of the pulse is transmitted past the boundary. Figure 5 is a Mathematica-generated 3D plot that models a parabola-of-revolution-shaped bottle microresonator. Figure 6 left demonstrates the time evolution of a Gaussian-shaped wave pulse inside of a bottle microresonator. This model corresponds to the behavior of a harmonic oscillator potential.

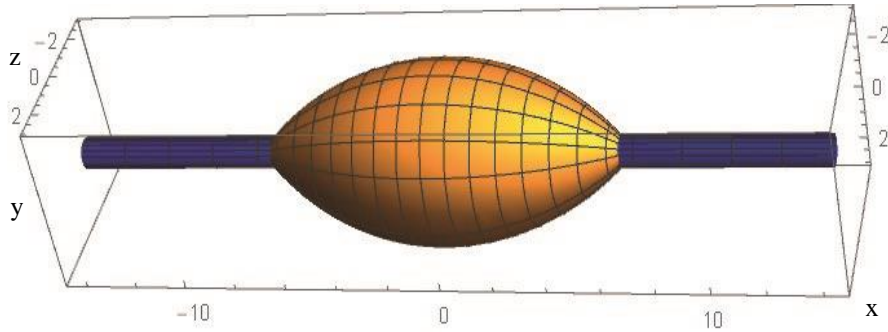


FIGURE 5. Graphic model of a bottle microresonator.

Figure 6, right, is a Gaussian pulse in a finite square well. Once again, this Mathematica-generated image simulates the pulse propagating radially around the cylindrical microresonator. The image is generated for time $[0, 0.15]$, instead of $[0, 0.4]$ as in Fig. 6, because Mathematica lacks the processing power to adequately simulate the pulse after it reflects off the boundary of the microresonator once. This simulation is less idealized than the infinite square well, and thus, part of the pulse is transmitted through the boundary each time that the pulse reflects off the side of the microresonator.

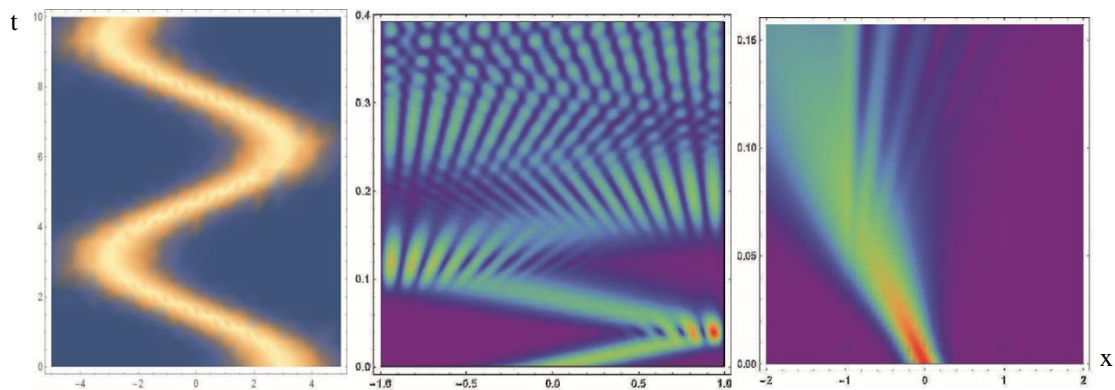


FIGURE 6. Left: Time evolution of a Gaussian-shaped wave pulse inside a parabola-of-revolution-shaped bottle microresonator. This corresponds to a harmonic oscillator potential. Middle: Gaussian in an infinite square well. Right: Gaussian in a finite square well.

WHERE TO FIND FURTHER INFORMATION

Dr. M. Sumetsky's paper "Microscopic Optical Buffering in a Harmonic Potential" gives greater detail on the link between a one-dimensional harmonic potential and the manufacturing of an optical buffer.⁴ Further information on SNAP devices can be found in Dr. M. Sumetsky and Dr. Y. Dulashko's paper "SNAP: Fabrication of Long Coupled Microresonator Chains with Sub-Angstrom Precision."⁷

ACKNOWLEDGMENTS

I would like to first acknowledge the Army Research Labs (ARL) team of Dr. Brian Kirby, Dr. Dash Vituello, and Dr. M. Sumetsky for their extensive work on the topic and willingness to teach me the material during my visit to ARL. I also want to express gratitude for my USMA research adviser, Dr. Michael Pfenning, for educating and assisting me throughout the entire research process. I want to thank Army Research Labs and the USMA Photonics Research Center for making this joint project possible.

REFERENCES

1. A. M. Weiner, *Ultrafast Optics* (John Wiley & Sons, New York, 2009).
2. D. Griffiths, *Introduction to Quantum Mechanics*, 2nd ed. (Pearson, New York, 2005).
3. E. Schrödinger, *Collected Papers on Wave Mechanics*, 3rd ed. (AMS Chelsea Publishing, American Mathematical Society, Providence, RI, 2003).
4. M. Sumetsky, *Sci. Rep.* **22**(5), 18569 (2015).
5. A. B. Matsko and V. S. Ilchenko, *IEEE J. Sel. Topics Quantum Electron.* **12**(1), 3–14 (2006).
6. G. C. Righini, Y. Dumeige, P. Féron, M. Ferrari, G. Nunzi Conti, D. Ristic, and S. Soria, *Riv. Nuovo Cimento* **34**(7), 435–488 (2011).
7. M. Sumetsky and Y. Dulashko, *Opt. Express* **20**(25), 27896–27901 (2012).
8. M. Sumetsky, *Nanophotonics* **2**(5-6), 393–406 (2013).
9. L. A. Kochkurov and M. Sumetsky, *Opt. Lett.* **40**(7), 1430–1433 (2015).